Supplementary Materials

Drug delivery nanoparticles for preventing implant bacterial infections based on the bacteria and immunity mechanisms

Chen Chen ‡[a], Qi Xiao ‡[a], Leyi Xiao[a], Mengge Feng[a], Fangzhe Liu[a], Ke Yao[a], Yu Cui[a], Tiange Zhang[a], Yufeng Zhang[a, b, c, *]

a, State Key Laboratory of Oral & Maxillofacial Reconstruction and Regeneration, Key Laboratory of Oral Biomedicine Ministry of Education, Hubei Key Laboratory of Stomatology, School & Hospital of Stomatology, Wuhan University, Wuhan University, Wuhan 430079, China.

b, Frontier Science Center for Immunology and Metabolism, Wuhan University, Wuhan 430071, China.

c, TaiKang Center for Life and Medical Sciences, Wuhan University, Wuhan 430071, China.

*Corresponding author E-mail: zyf@whu.edu.cn

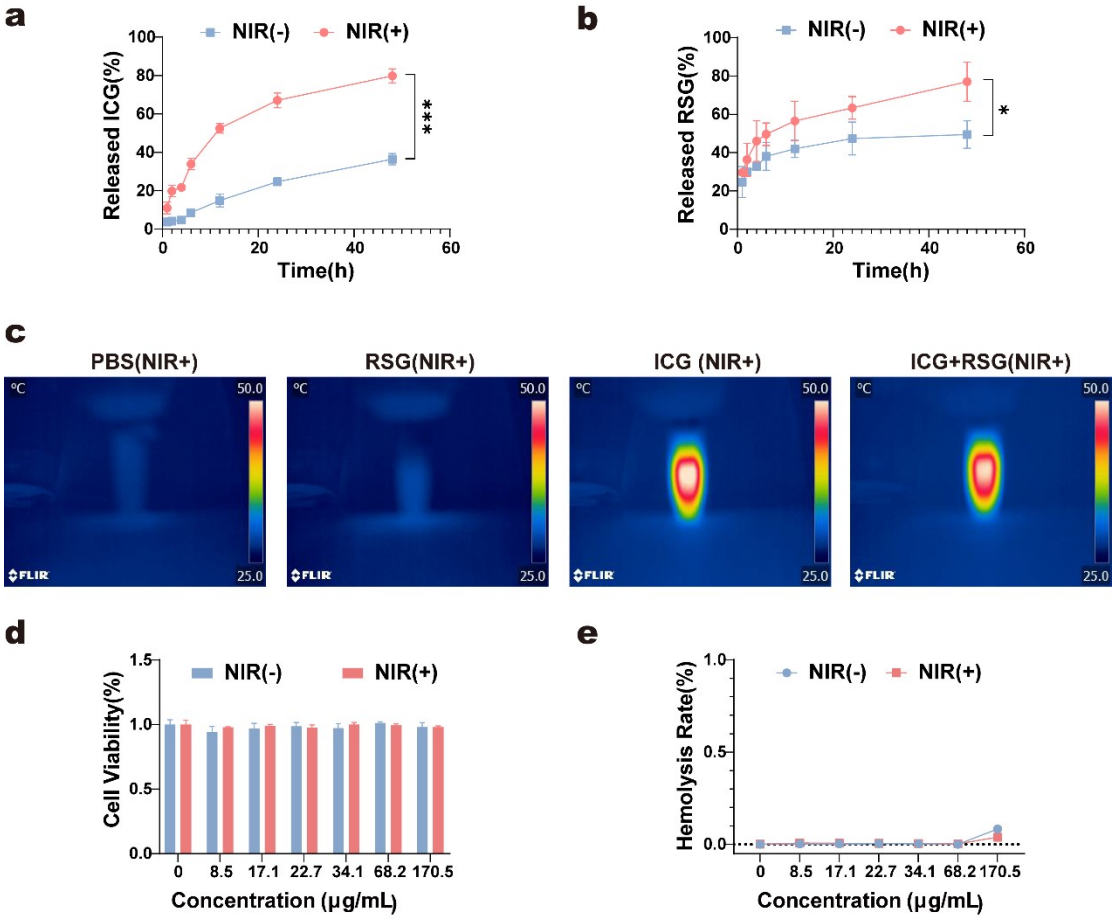

Figure S1. a) Release curves of ICG. b) Release curves of RSG. c) Photothermal images of four groups under 808nm laser. d) Cell viability of NH3T3 cells treated with ICG+RSG in various concentrations and light conditions. e) Hemolytic toxicity assessment in various concentrations and light conditions. Data are presented as mean ± SD (n = 3). *P < 0.05, **P < 0.01, and ***P < 0.001.

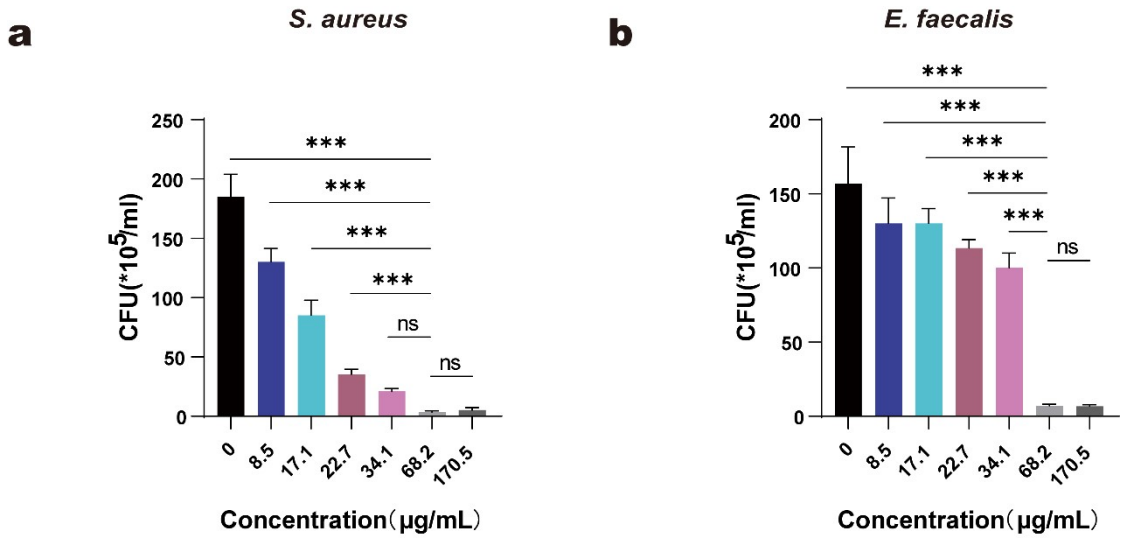

Figure S2. Antibacterial effect of different ICG+RSG concentrations. Data are presented as mean ± SD (n = 3). *P < 0.05, **P < 0.01, and ***P < 0.001.

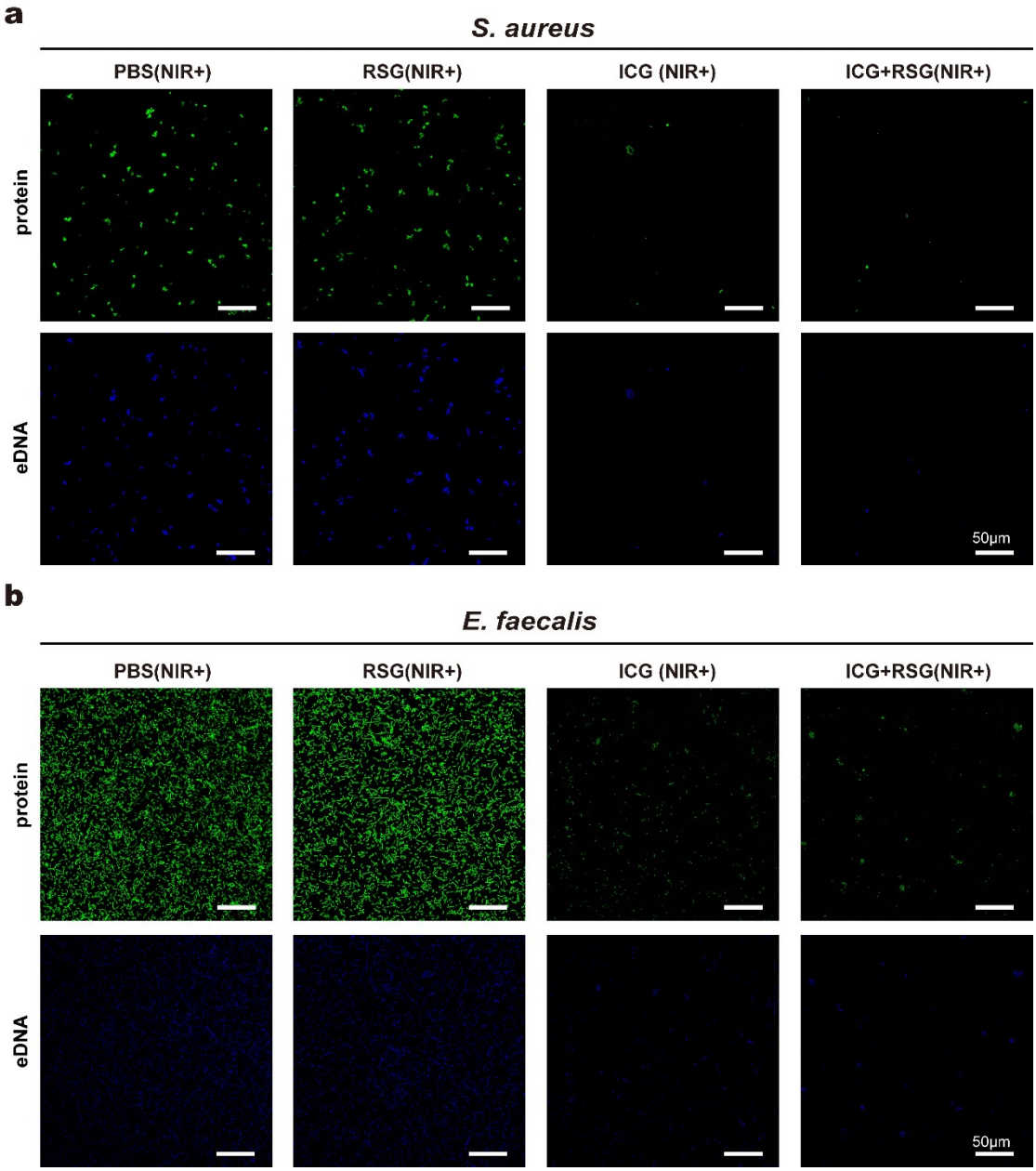

Figure S3. a) Confocal microscopy images of proteins and eDNA from *S. aureus* biofilms. b) Confocal microscopy images of proteins and eDNA from *E. faecalis* biofilms.

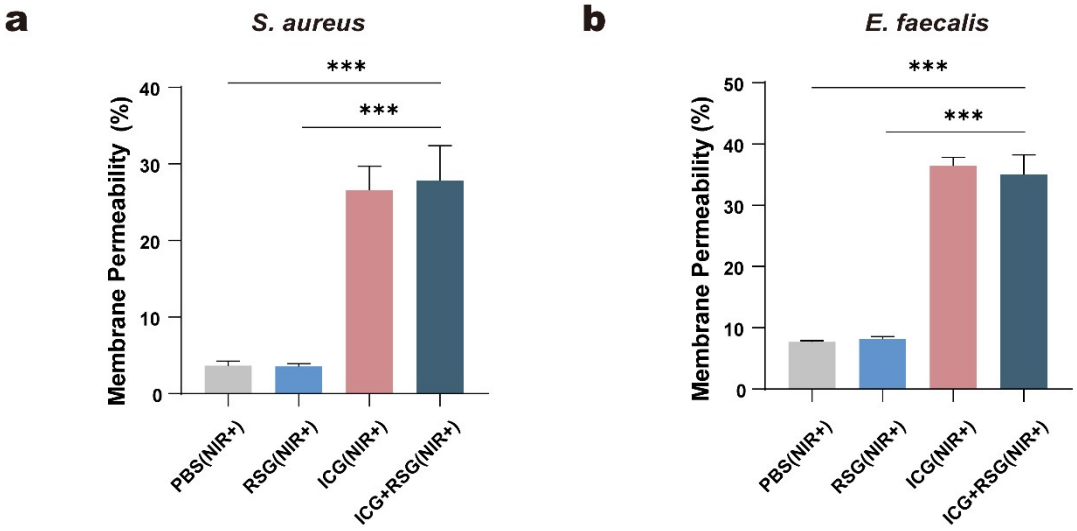

Figure S4. a) Cell plasma membrane permeability proportion of *S. aureus*. b) Cell plasma membrane permeability proportion of *E. faecalis*. Data are presented as mean ± SD (n = 3). *P < 0.05, **P < 0.01, and ***P < 0.001.

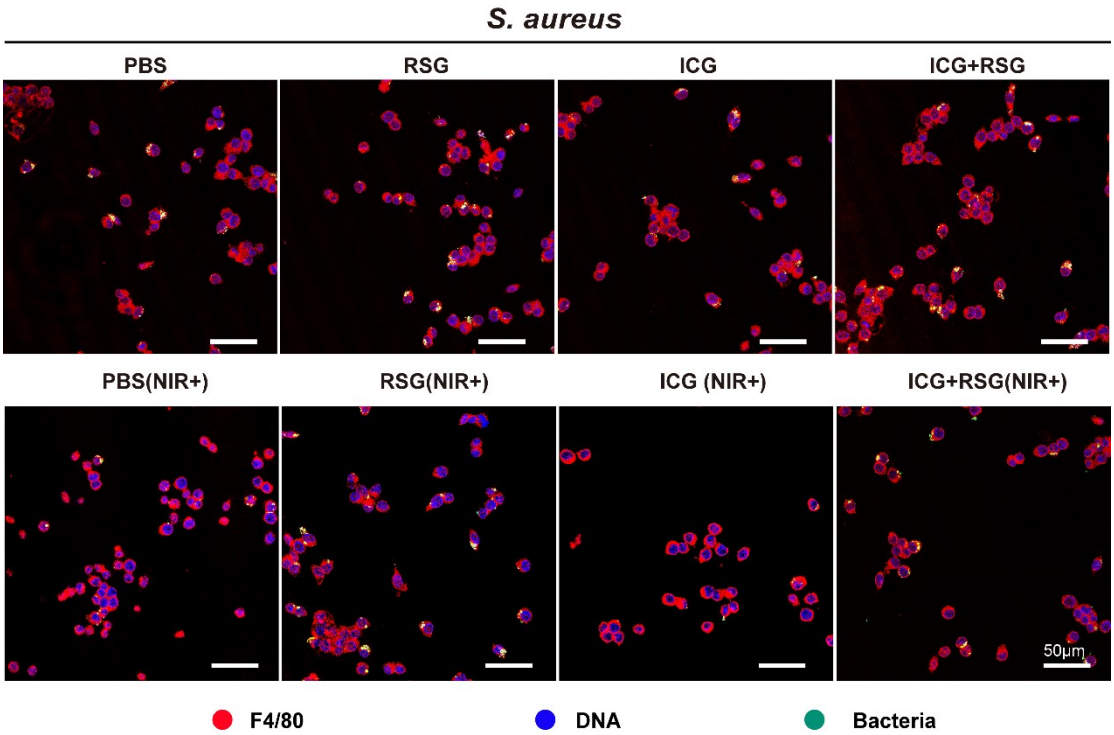

Figure S5. Immunofluorescence images of phagocytosis of *S. aureus* by RAW264.7 cells. (scale bar = 50 μm). Red: F4/80; Blue: DNA; Green: Bacteria.

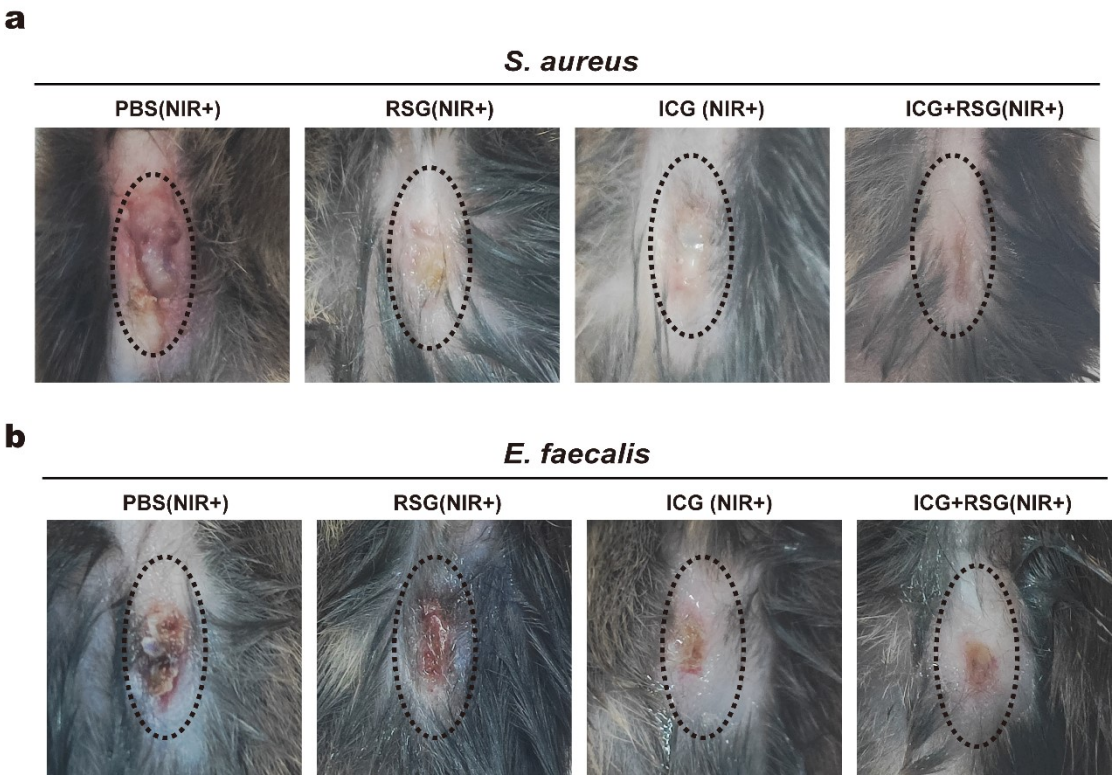

Figure S6. a) Photographs of healing skin incisions in four groups of mice treated with *S. aureus*. b) Photographs of healing skin incisions in four groups of mice treated with *E. faecalis*.

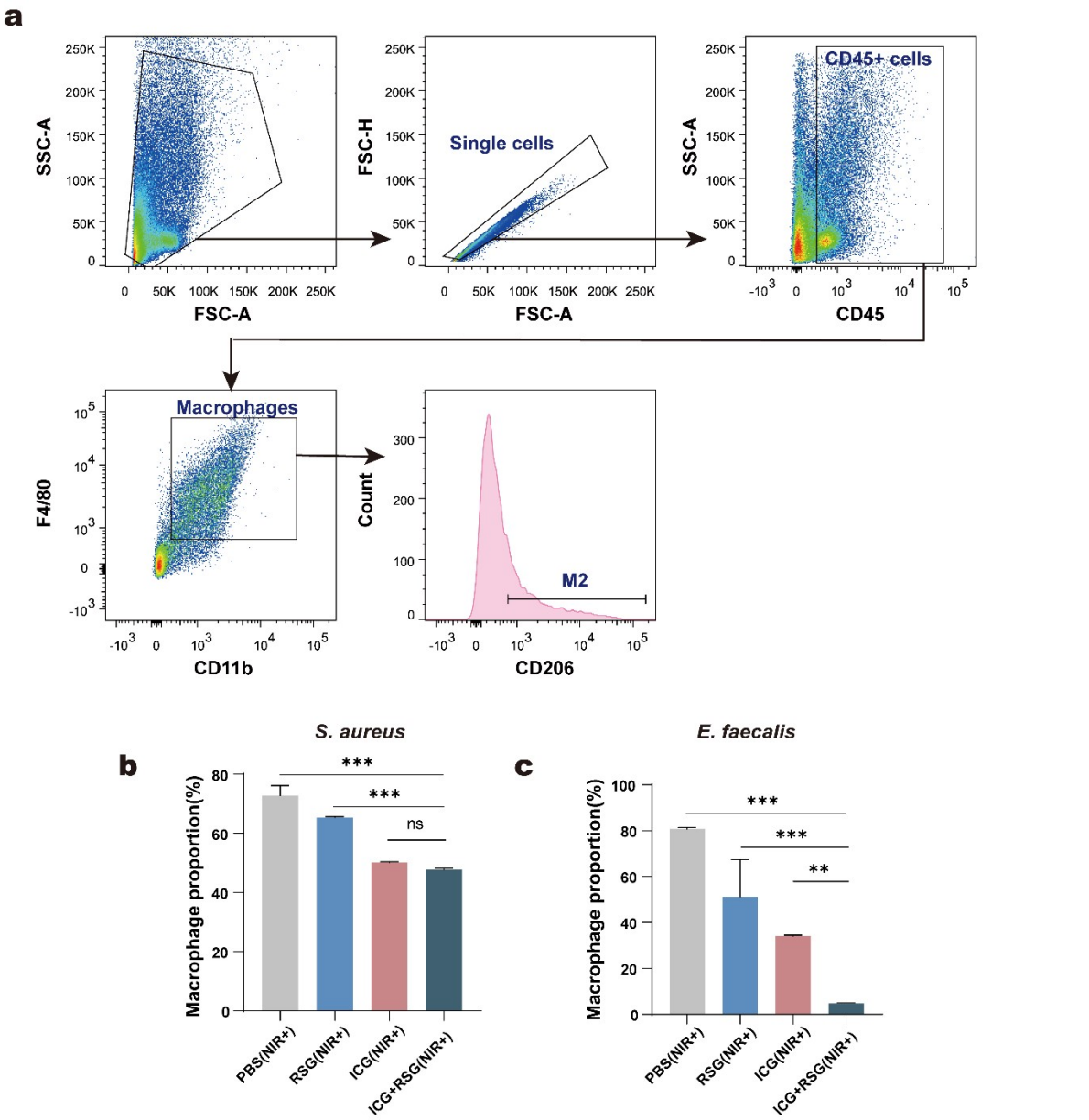

Figure S7. a) Flow cytometry circle-gate strategy for M2 macrophages. b, c) Proportion of macrophages in four groups of mice under two bacterial infections Data are presented as mean ± SD (n = 3). *P < 0.05, **P < 0.01, and ***P < 0.001.

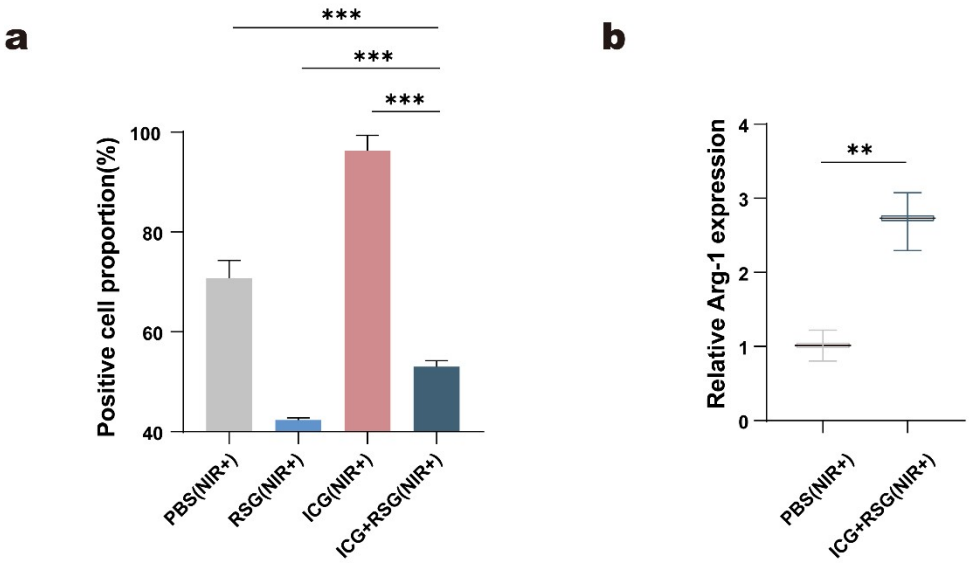

Figure S8. a) Changes in ROS levels of RAW264.7 under different treatments detected by flow cytometry. b) Relative mRNA level of Arg-1. Data are presented as mean ± standard deviation (n = 3). *p < 0.05, **p < 0.01, and ***p < 0.001.

Table S1. The primer sequences used for qRT-PCR.

Gene	Forward (5'-3')	Reverse (5'-3')
GAPDH	TGACCACAGTCCATGCCATC	GACGGACACATTGGGGGTAG
Arg-1	CATTGGCTTGCGAGACGTAGA C	GCTGAAGGTCTCTTCCATCAC C

Table S2. Encapsulation efficiency of three groups nanoparticles.

group	EE of RSG	EE of ICG
RSG	45.5±5.4%	-
ICG	-	69.4±1.2%
ICG+RSG	56.0%±4.4%	74.6%±1.4%

Data are presented as mean ± standard deviation (n = 3).